tvst

Article

Relief of Cystoid Macular Edema-Induced Focal Axonal Compression with Anti-Vascular Endothelial Growth Factor Treatment

Eyyup Karahan[1,2], Aliaa Abdelhakim[1], Ceren Durmaz[1,3], and Tongalp H. Tezel[1]

[1] Department of Ophthalmology, Columbia University, Vagelos College of Physicians and Surgeons, New York, NY, USA
[2] Department of Ophthalmology, Balikesir University, Balikesir, Turkey
[3] Department of Ophthalmology, Dokuz Eylul University, Izmir, Turkey

Correspondence: Tongalp H. Tezel, Harkness Eye Institute, Department of Ophthalmology, Columbia University, Vagelos College of Physicians and Surgeons, 635 West 165th Street, New York, NY 10032, USA. e-mail: tht2115@cumc.columbia.edu

Received: June 7, 2019
Accepted: December 7, 2019
Published: March 18, 2020

Keywords: macular edema; anti-VEGF treatment; optical coherence tomography; image analysis; ganglion cells; axonal compression

Citation: Karahan E, Abdelhakim A, Durmaz C, Tezel TH. Relief of cystoid macular edema-induced focal axonal compression with anti-vascular endothelial growth factor treatment. Trans Vis Sci Tech. 2020;9(4):18, https://doi.org/10.1167/tvst.9.4.18

Purpose: To evaluate the mechanical compression of retinal nerve fiber layer (RNFL) by intraretinal cysts in macular edema and its relief with anti-vascular endothelial growth factor (anti-VEGF) treatment.

Methods: Optical coherence tomography scans were used to measure RNFL thickness and reflectance at seven preselected points at and around the peak of the edema before and after anti-VEGF treatment in 10 patients (11 eyes) with branch retina vein occlusion (BRVO) and diabetic macular edema (DME). Scans through nonedematous retina and from the fellow eyes were taken as controls. Correlations were sought between the changes in retinal and RNFL thickness, RNFL reflectance, and the size of the intraretinal cysts.

Results: Postinjection RNFL thickness decreased significantly only at peak point of the edema (18.1 $\pm$ 2.7 vs. 13.8 $\pm$ 1.2 µm; $P = 0.038$), at its nasal edge (20.1 $\pm$ 2.7 vs. 15.5 $\pm$ 1.4 µm; $P = 0.026$), and 500 µm away from its nasal border (35.7 $\pm$ 6.0 vs. 20.1 $\pm$ 2.7 µm; $P = 0.006$) suggesting focal stagnation of the axoplasmic flow owing to compression at its peak point. Significant postinjection decreases in RNFL reflectivity were also noted at peak point of the cyst (164.9 $\pm$ 10.3 vs. 141.5 $\pm$ 12.6 arbitrary units [AU]; $P = 0.037$), at its nasal edge (166.8 $\pm$ 7.8 vs. 135.1 $\pm$ 10.2 AU; $P = 0.02$), and 1500 µm away from temporal edge (160.2 $\pm$ 6.2 vs. 141.1 $\pm$ 6.4 AU; $P = 0.022$). Cyst proximity to RNFL ($D_{50} = 50$ µm) was the only determinant significantly affecting the magnitude of the RNFL thickness change after anti-VEGF treatment ($P = 0.001$).

Conclusions: Intraretinal cysts due to BRVO and DME locally compress overlying axons and induce anatomic changes suggestive of axoplasmic stagnation. This compression can be relieved with anti-VEGF treatment.

Translational Relevance: Focal compression of RFNL by retinal cysts may indicate a need for early treatment of macular edema to prevent axonal loss, especially in patients with low axonal reserve

Introduction

Anti-vascular endothelial growth factor (anti-VEGF) therapy has become the standard of care for macular edema associated with diabetic retinopathy and retinal vein occlusion. The 2018 Preferences and Trends Survey (https://www.asrs.org) revealed that intravitreal anti-VEGF drugs are the first line of treatment in 95.7% of cases with diabetic macular edema (DME), and 98.7% of the branch retinal vein occlusion cases presenting with cystoid macular edema. Anti-VEGF agents neutralize the VEGF-A, which is responsible for angiogenesis and vascular leakage.[1] However, VEGF-A also exerts a neuroprotective effect on retinal neurons,[2,3] particularly on retinal ganglion cells.[4,5] Inhibition of VEGF-A raises the possibility of abolishing this protective effect. Several clinical studies,[6,7] supported by in vitro experiments[8,9] and animal models of retinal diseases,[10] indicate that

neutralization of VEGF may be harmful to retinal ganglion cells. These findings have recently been challenged with experimental data[11] and meta-analysis of clinical studies[12,13] that fail to show any cytotoxic effect of anti-VEGF drugs on retinal ganglion cells and retinal nerve fiber layer (RNFL). These controversial views have recently been the subject of discussions in interpreting the latest findings of the Diabetic Retinopathy Clinical Research Network Group, which showed that, in comparison to panretinal photocoagulation, anti-VEGF therapy appeared to cause more RNFL thinning over the course of a 2-year period.[14] Authors attributed their observation to resolution of RNFL edema rather than loss of RNFL axons.

Although much of the focus on RNFL structural changes has been centered on the role that anti-VEGF therapies play, one factor that has not been investigated in detail is the role played by volumetric expansion of the intraretinal macular cysts on the overlying RNFL. The physical strain caused by intraretinal cysts can result in RNFL compression and deformation, which may in turn slow down or even halt the axoplasmic flow. Focal compression of axon is known to result in accumulation of large numbers of mitochondria at the obstruction site, which deteriorates the axoplasmic flow further and cause distention[15] and hyperreflective appearance of the axonal segment around the constriction point on optical coherence tomography (OCT).[16,17] The magnitude of the pressure exerted on the RNFL by gradually expanding intraretinal fluid pockets has never been estimated; however, it must be greater than the intraocular pressure to distend the inner retina toward the vitreous cavity against the intraocular pressure. Thus it is reasonable to speculate that at the peak point of cystoid macular edema, pressures exceeding the intraocular pressure focally compress retinal ganglion cell axons. Although increases in RNFL thickness and resultant interruptions in axonal transport are well documented in other acute compressive pathologies, such as papilledema[18] and acute angle closure glaucoma,[19] the acute focal compression and axonal stasis that would theoretically result from cystic expansion and physical strain on the RNFL from macular edema has not been explored.

Herein we hypothesized that like other compressive neuropathies, macular edema would cause changes in thickness and reflectance of the neighboring RNFL area in a focal manner, and that these topographic changes would resolve with anti-VEGF therapy. Similar to other compressive neuropathologies, macular edema would likely result in an interruption of axonal transport systems of the RNFL axons, which would lead to axonal swelling and pooling of hyper-reflective cytoskeletal cargo, including subcellular organelles, such as mitochondria, proteins, and neurovesicles.[20,21] Unlike global compressive pathologies, however, the changes in the RNFL would likely be limited to the immediate environs of the macular cysts. To test these hypotheses, we sought to measure topographic changes in thickness and reflectance of the RNFL overlying areas of macular edema, and to compare these measurements before and after anti-VEGF therapy.

Methods

This interventional retrospective case analysis was approved and monitored by the institutional review board of the Columbia University, Vagelos College of Physicians and Surgeons, and conducted according to the principles of the Declaration of Helsinki. Informed consent was obtained from each patient prior to intravitreal injection.

Study Subjects and Inclusion Criteria

Clinical files and retinal imaging studies of 43 patients with cystoid macular edema secondary to branch retinal vein occlusion and 74 patients with clinically significant DME in the setting of mild to severe nonproliferative diabetic retinopathy (severity levels 35–53 according to ETDRS [Early Treatment of Diabetic Retinopathy Study] classification)[22] were screened retrospectively. Only subjects who had undergone fluorescein angiography within 2 weeks prior to intravitreal anti-VEGF injection, and had spectral domain OCT scanning (Spectralis; Heidelberg Engineering GmbH, Heidelberg, Germany) of the macula within 2 weeks before and 4 to 10 weeks after the injection were included into the screening process. The follow-up period of the patients was limited to <10 weeks to prevent disease-specific factors, that is, ischemia, neuropathy, or intraocular pressure increases, from confounding the analyses and interpretation of the results. More than 2 months from the last anti-VEGF injection was required for inclusion into the study.

Strict eligibility criteria were applied to eliminate any confounding factors, including media opacities, high myopia (>6 D), glaucoma, ocular hypertension (intraocular pressure >21 mm Hg),[23] retinal surgery or laser, recent (<4 months) eye surgery, corneal graft, ocular injury, intraocular inflammation, macular degeneration, inherited retinal degenerations, macular scars, epiretinal membrane, vitreomacular traction, previous intravitreal steroid injections, and

any other neurodegenerative disease. Because repeated injections of intravitreal anti-VEGF agents are associated with chronic ocular hypertension,[24] eyes receiving more than seven intravitreal injections, which are at higher odds of developing ocular hypertension, were excluded.[25,26]

Macular perfusion status of the patients was assessed by two masked graders (EK and THT) using the fluorescein and/or OCT angiography (AngioPlex; Carl Zeiss Meditec, Inc., Dublin, CA). Eyes with mild to severe macular ischemia[27] were excluded. Intraclass correlation coefficient for identifying "absent" or "questionable" level of macular ischemia was 0.95.

During each visit, patients underwent a full ocular examination with determination of best-corrected Snellen visual acuity, applanation tonometry, slit lamp examination of the anterior segment, and binocular assessment of the posterior segment. During the study period patients received one intravitreal injection of either bevacizumab (Avastin; 1.25 mg/50 µL, Genentech, South San Francisco, CA), or aflibercept (Eylea; 2.0 mg/50 µL, Regeneron, Tarrytown, NY). An experienced retinal specialist (THT) gave the intravitreal injection at the superotemporal quadrant 3 mm away from the limbus. Povidone-iodine, topical antibiotics, and an eye speculum were used as part of the preinjection procedure. Binocular indirect fundus examination was done immediately following each injection. Clinical examination and OCT imaging was repeated 6 to 8 weeks after the intravitreal anti-VEGF injection.

Image Acquisition and Analyses

Because of the known variability of RNFL thickness measurements with different OCT devices,[28] only patients imaged with spectral-domain Spectralis OCT (Heidelberg Engineering GmbH) were included in the study. This device can perform 40,000 A-scans per second with 3.5-µm digital axial resolution. Images were acquired using image alignment eye-tracking software (TruTrack; Heidelberg Engineering GmbH). For each patient, 49 horizontal scans covering a 6 × 6 mm^2 (20°) area centered at the fovea were obtained using Family Acquisition Module 6.5.2.0. B-scan averaging was set at 16 frames for noise reduction while the eye-tracking system was maintaining the stability of the image. Because of the known interference of macular edema on OCT signal strength, only images with a signal strength of >20 db were used in further analyses.[29] Borders of the area of macular edema and the location of its peak point (P) were determined from the three-dimensional macular map reconstruction using horizontal raster scans. The distance of the peak point of the edematous retina to the foveola was determined using the inbuilt caliper of the OCT device. Horizontal scans across the peak point were used for further image analyses.

Captured OCT scans were manually segmented into two zones by tracing the borders of the following: (1) inner border of the inner limiting membrane; (2) outer border of the RNFL; and (3) outer border of the fourth hyperreflective line of the outer retina, which corresponds to retinal pigment epithelium (RPE)-Bruch's membrane complex. The area between in the inner border of the internal limiting membrane and the outer border of the RNFL was accepted as the "RNFL zone," whereas the area between the outer borders of the RNFL and RPE-Bruch's membrane complex was defined as "subRNFL zone." Images were then exported to ImageJ software (http://rsb.info.nih.gov/ij/) and converted to 8-bit grayscale images for better visualization and further processing. Seven prespecified linearly arranged points along the horizontal line scan crossing through the foveola and the area of cystic change within the macula were used to measure the RNFL thickness and reflectivity (Fig. 1). These loci were:

(1) The peak point of the macular edema (P),
(2) The nasal edge of the macular edema (N),
(3) The temporal edge of the macular edema (T),
(4) 500 µm nasal from the nasal edge of the macular edema (N500),
(5) 1500 µm nasal from the nasal edge of the macular edema (N1500),
(6) 2500 µm nasal from the nasal edge of the macular edema (N2500),
(7) 1500 µm temporal to the temporal edge of the macular edema (T1500).

RFNL thickness and reflectance measurements were done before and after anti-VEGF injection at and 10 µm nasal and temporal side of predetermined points, and the average value for each point was calculated. Because of its consistency among individuals, the diameter of the superotemporal vein at the parapillary border was accepted as 125 µm[30] and used for spatial calibration.

For reflectance analyses, the pixels corresponding to the boundary marks were considered to be a part of the segment below the boundary line. Intensity plot profiles revealing the reflectance values of RNFL and subRFNL zones were then extracted. Reflectance values at 10 µm nasal and temporal sides of each predetermined point were averaged to yield the RNFL and subRFNL reflectance value for that point. To minimize the impact of optical differences, RNFL reflectance values at each point were normal-

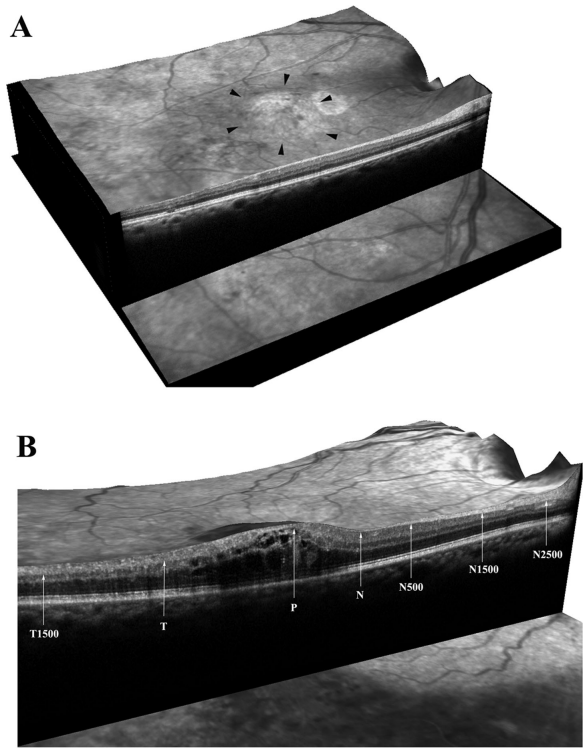

Figure 1. (A) Three-dimensional contour of the macular edema was inspected to determine the borders of the edematous retina and the location of the peak point (P). (B) Horizontal OCT scans passing through the peak point were used to calculate the RNFL and retina thickness, as well as RNFL reflectivity at seven preselected points, namely, the peak of the macular edema (P), its nasal (N) and temporal (T) edges, and 500 (N500), 1500 (N1500), and 2500 (N2500) µm away from its nasal edge, as well as at a point 1500 µm away from the temporal edge (T1500) of the macular edema. The borders of the RNFL, sensory retina, and intraretinal cysts were manually delineated.

ized by dividing the mean RNFL reflectance value to the reflectance value of the subRFNL zone at that location (=RNFL/subRNFL). This normalization was shown to yield the lowest variation compared with other normalization techniques.[31] Comparing RNFL reflectance before and after the anti-VEGF injection at each point required further consideration for the possible reflectance increases in the subRFNL zones after the resolution of the intraretinal cysts. For this purpose, the impact of intraretinal cyst resolution on the reflectance of the optical segments below the RNFL was analyzed. The change of reflectance in the subRFNL zone was calculated for each study point and expressed as the quotient (Q) of the subRFNL reflectance value before and after anti-VEGF treatment (Q = subRFNL reflectance after anti-VEGF/subRFNL reflectance before anti-VEGF). This quotient was used to correct the normalization of the RNF/subRFNL reflectance ratio as is seen in the following formula:

$$\frac{RNFL\ Reflectance\ after\ antiVEGFInjection}{SubRNFL\ Reflectance\ after\ antiVEGF\ Injection} \times (Q) \times \left(\frac{1}{k}\right)$$

To unveil the impact of cystoid macular edema on RNFL, similar calculations were done on two horizontal OCT scans within the same meridian but passing through the nonedematous portion of the macula. We often used the horizontal scans crossing through the superior and inferior borders of the optic nerve. If one of these horizontal internal control scans coincide with the area of macular edema, such as in the case of branch retinal vein occlusion, only one horizontal scan was used. The ratio of the RNFL thickness and reflectance changes at predetermined loci within the macular edema were also corrected to the changes at corresponding points (k) along the horizontal scan passing through nonedematous retina to minimize the impact of any possible disease-specific process or direct anti-VEGF–related impact on measured parameters, and thus isolate the impact of mechanical compression on the axons.

Calibrated OCT scans were used to calculate the closest distance of the intraretinal fluid pockets to RNFL, as well as the total cyst area, which is defined as the summation of the areas of all intraretinal fluid pockets.

Correlations between the structural characteristics of the intraretinal cysts and the amount of RNFL thinning after anti-VEGF treatment were also investigated to determine whether there are any anatomic features of the macular cysts that can be predictive of the amount of RNFL thickening and subsequent postinjection thinning. For this purpose, adjacent intraretinal fluid pockets were conjoined manually and treated as a single cyst. Correlation analysis was conducted to determine whether RNFL thickness changes after anti-VEGF injection were impacted by the total cyst area, the proximity of the cystic apex at the peak point (P) to RNFL, vertical and horizontal diameters of the intraretinal fluid pockets, as well as the total thickness of the retina and RNFL reflectance.

Statistical Analyses

All quantitative data were expressed as mean ± standard error. Statistical analyses were performed using PASW Statistics software version 18.0 (SPSS Inc., Chicago, IL). Changes in visual acuity, intraocular pressures, and temporal variations of the RNFL thickness and reflectance at predetermined loci were analyzed using the Wilcoxon signed-rank test. Correlation analysis was performed using the Spear-

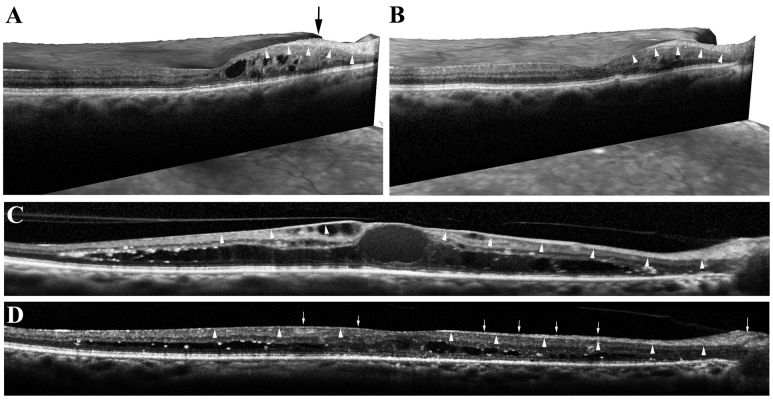

Figure 2. (A) Three-dimensional OCT scan of an 86-year-old male patient with inferotemporal branch retinal vein occlusion in the right eye. Patient developed macular edema with a peak located 1900 µm nasal to the fovea (*black arrow*). RNFL is thickened and displays high reflectivity (*white arrowheads*). (B) Four weeks after intravitreal bevacizumab injection, a horizontal scan from the same meridian reveals resorption of the intraretinal cysts along with a 12.3% decrease in retinal thickness at the peak point (600–525.3 µm). A higher (23.2%; 120–92.1 µm) reduction in RNFL thickness with a decrease in its reflectivity was also observed (*white arrowheads*). (C) Horizontal line scan through the peak point of the clinically significant DME in the right eye of a 65-year-old female patient. The peak point of the edema was located 5.5 µm nasal and 167.8 µm inferior to the foveola. A diffuse thickening and increased reflectance of the RNFL around the peak point is seen (*white arrowheads*). (D) Four weeks after an intravitreal aflibercept (2.0 mg/50 mL) injection patient's visual acuity improved from 20/100 to 20/70 along with disappearance of most of the intraretinal cysts. A marked reduction of the RNFL around the peak point was accompanied by loss of diffuse reflectance of the RNFL. At this point, occasional hyperreflective small dots (*white arrows*) are observed within the RNFL, which may represent aggregates of macromolecules within the axoplasm.

man rank-order correlation test between the magnitude of change in RNFL thickness at preselected loci after anti-VEGF treatment against patients' age, change in the area, vertical and horizontal diameters of the cysts, closest distance of cysts to RNFL, changes in RNFL intensity, and change in total retinal thickness. Impact of anti-VEGF treatment on percent change of RNFL thickness and reflectance was analyzed using the Kruskal–Wallis one-way analysis of variance on ranks, and differences between predetermined loci was sought with the Student–Newman–Keuls multiple comparison test. A confidence level of $P < 0.05$ was considered to be statistically significant.

Results

Seventy-four patient with DME and 43 patients with macular edema secondary to branch retinal vein occlusion were screened for analysis. Only 11 eyes of 10 patients (5 men and 5 women) were eligible for the study. Exclusion reasons are given in Supplemental Table S1. Five patients (6 eyes) had DME and 5 patients (5 eyes) had cystoid macular edema secondary to branch retinal vein occlusion. The mean age of the patients was 69 ± 2.4 (55–86) years. Nine eyes were treated with bevacizumab, and two eyes were treated with aflibercept. Mean number of previous intravitreal injections were 3.1 ± 1.2. Mean follow-up after the anti-VEGF injection was 47 ± 8 (30–66) days. Visual acuity of all patients (average preinjection: 20/92 ± 20/24) improved significantly after anti-VEGF injection (20/55 ± 20/23; $P < 0.001$). Mean preinjection intraocular pressure (16.7 ± 1.0 mm Hg, 10–20 mm Hg) remained the same after the injection (16.5 ± 0.9 mm Hg, 10–20 mm Hg; $P = 1.0$).

The peak point of the macular edema was 535.9 ± 128.2 µm away from the fovea (472.6 ± 52.1 µm for eyes with DME vs. 611.9 ± 191.1 µm for eyes with macular edema secondary to retinal vein occlusion; $P = 0.93$). In only one eye, the peak point was at the foveola. In 6 of 11 (54.5%) eyes the peak point was located nasal to the fovea, and in 7 of 11 eyes it was above the fovea (Fig. 2). The total area (51,919 ± 2,296 µm^2 vs. 7,082 ± 1,202 µm^2; P =0.03), vertical (168.7 ± 4.4 µm vs. 35.4 ± 3.3 µm; $P = 0.03$), horizontal (360.3 ± 15.3 µm vs. 105.6 ± 15.3 µm; P = 0.03), and average (264.5 ± 7.1 µm vs. 70.5 ± 9.0 µm; $P = 0.03$) diameters of the intraretinal cysts decreased significantly after anti-VEGF treatment (Table 1).

No correlation was found between the number of previous anti-VEGF injections and the initial RNFL thicknesses and reflectance at preselected points ($P > 0.05$). After anti-VEGF injection, RNFL thickness demonstrated significant decrease ($P < 0.05$). Multiple comparison analyses revealed that there were significant differences in the amount of RNFL

Table 1. Change in OCT Features of Retina with Resolution of Diabetic Macular Edema

OCT Parameters	Before Anti-VEGF	After Anti-VEGF	*P* Value
Total area of the cysts (μ^2)	51,919 ± 2,296	7,082 ± 1,202	0.003*
Distance of cyst to RNFL (μ)	92.3 ± 5.1	156.3 ± 5.3	0.003*
Horizontal diameter of the cysts (μ)	360.3 ± 15.3	105.6 ± 15.3	0.003*
Vertical diameter of the cysts (μ)	168.7 ± 4.4	35.4 ± 3.3	0.003*
Average diameter of the cysts (μ)	264.5 ± 7.1	70.5 ± 9.0	<0.001*
RNFL thickness at point P (μ)	18.1 ± 2.7	13.8 ± 1.2	0.038*
RNFL thickness at point N (μ)	20.1 ± 2.7	15.5 ± 1.4	0.026*
RNFL thickness at point N500 (μ)	35.7 ± 6.0	20.1 ± 2.7	0.006*
RNFL thickness at point N1500 (μ)	43.5 ± 5.6	41.3 ± 5.5	0.594
RNFL thickness at point N2500 (μ)	84.6 ± 11.6	83.3 ± 12.5	0.722
RNFL thickness at point T (μ)	16.6 ± 1.3	14.5 ± 1.2	0.328
RNFL thickness at point T1500 (μ)	15.6 ± 0.9	14.3 ± 1.3	0.167
RNFL reflectance at point P (AU)	164.9 ± 10.3	141.5 ± 12.6	0.037*
RNFL reflectance at point N (AU)	166.8 ± 7.8	135.1 ± 10.2	0.02*
RNFL reflectance at point N500 (AU)	170.8 ± 6.4	152.4 ± 8.7	0.052
RNFL reflectance at point N1500 (AU)	182. 5 ± 5.7	173.5 ± 9.7	0.336
RNFL reflectance at point N2500 (AU)	174.6 ± 7.3	167.1 ± 9.0	0.277
RNFL reflectance at point T (AU)	154.4 ± 10.4	143.7 ± 11.3	0.286
RNFL reflectance at point T1500 (AU)	160.2 ± 6.2	141.1 ± 6.4	0.022*
Retinal thickness at point P (μ)	352.4 ± 20.5	245.4 ± 23.2	0.004*
Retinal thickness at point N (μ)	356.9 ± 18.9	252.9 ± 22.6	0.003*
Retinal thickness at point N500 (μ)	330.5 ± 18.2	252.5 ± 17.5	0.006*
Retinal thickness at point N1500 (μ)	241.9 ± 12.0	226.1 ± 10.9	0.594
Retinal thickness at point N2500 (μ)	226.7 ± 15.5	212.2 ± 13.1	0.075
Retinal thickness at point T (μ)	332.9 ± 22.4	233.1 ± 21.9	0.003*
Retinal thickness at point T1500 (μ)	203.2 ± 7.3	183.1 ± 7.3	0.062*

Mean ± SE.
AU = Arbitary Units.
*Wilcoxon signed-rank test.

decreases among seven predetermined points ($P < 0.001$) and the decrease in RNF thickness was significant at the peak point of cyst (P) (18.1 ± 2.7 vs. 13.8 ± 1.2 μm; $P = 0.038$), at its nasal edge (N) (20.1 ± 2.7 vs. 15.5 ± 1.4 μm; $P = 0.026$), and 500 μm nasal to the cyst (N500) (35.7 ± 6.0 vs. 20.1 ± 2.7 μm; $P = 0.006$) (Table 1; Figs. 3 and 4A). In contrast, no significant thinning was observed at 1500 μm (N1500) (43.5 ± 5.6 vs. 41.3 ± 5.5 μm; $P = 0.594$) and 2500 μm nasal to the cyst (N2500) (84.6 ± 11.6 vs. 83.3 ± 12.5 μm; $P = 0.722$), nor at the temporal edge of the cyst (T) (16.6 ± 1.3 vs. 14.5 ± 1.2 μm; $P = 0.328$) or 1500 μm temporal to the cyst (T1500) (15.6 ± 0.9 vs. 14.3 ± 1.3 μm; $P = 0.167$).

Compared with images immediately prior to anti-VEGF treatment, RNFL reflectance decreased significantly after the resolution of the cysts ($P < 0.05$). There were significant differences between seven observation points ($P < 0.001$) with the peak of the macular edema (P) (164.9 ± 34.2 vs. 141.5 ± 12.6 arbitrary units [AU]; $P = 0.037$), its nasal edge (N) (166.8 ± 7.8 vs. 135.1 ± 10.2 AU; $P = 0.02$), and 1500 μm temporal to the edema (T1500) (160.2 ± 6.2 vs. 141.1 ± 6.4 AU; $P = 0.022$) revealing marked decreases (Table 1; Figs. 3 and 4B). SubRNFL reflectance values did not change significantly after anti-VEGF treatment (1.01 ± 0.05 x; $P = 0.186$, Supplemental Figure 1) despite the resolution of the intraretinal cysts. Highest proportional subRFNL reflectance change after anti-VEGF treatment was observed at the peak point of the macular edema (P) (1.02 ± 0.04 x), but it remained nonsignificant compared with pretreatment values ($P = 0.193$). We calculated that 78.2% ± 5.6% of the reflectance values within the subRFNL zone

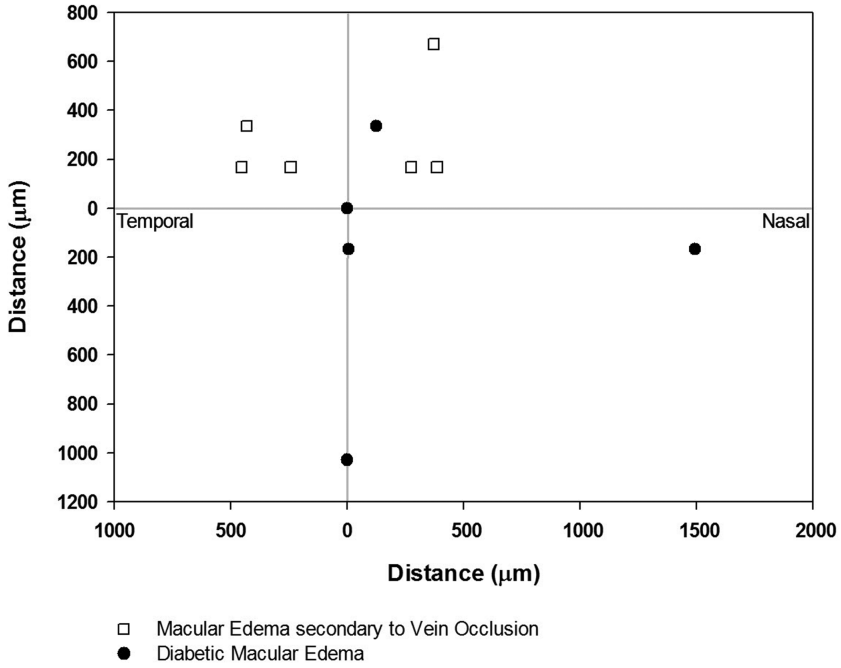

Figure 3. Distribution of the peak points (P) of the macular edema. Most of the peak points were located nasal (6 of 11 eyes, 54.5%) and superior (7 of 11 eyes, 63.6%) to the foveola. There was no difference in the proximity of the peak points to the foveola among eyes with macular edema secondary to diabetic retinopathy and branch retinal vein occlusion ($P = 0.93$).

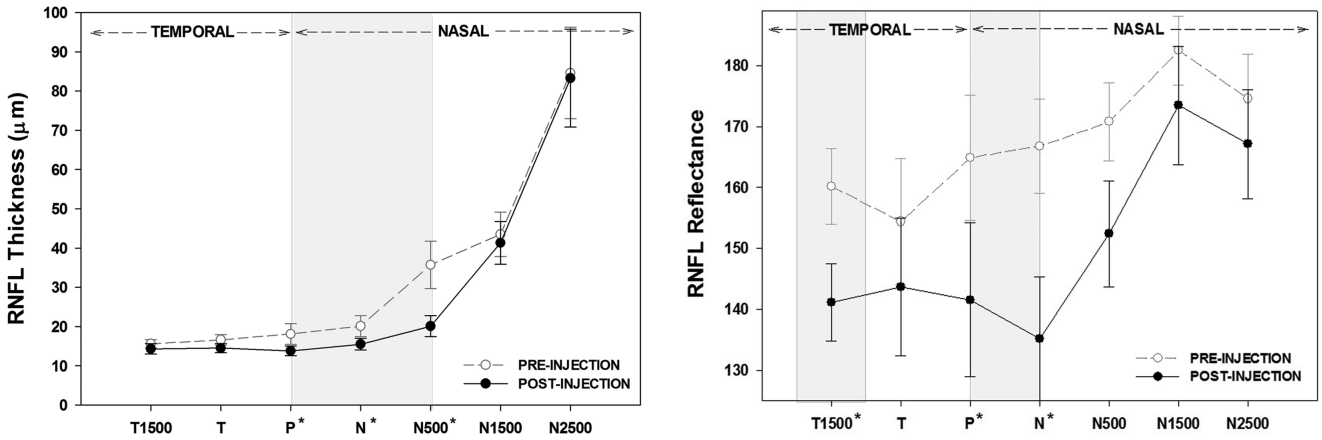

Figure 4. Change in RNFL thickness and reflectance after anti-VEGF treatment. Anti-VEGF treatment resulted in significant reduction in RNFL reflectance ($P < 0.001$) and thickness ($P < 0.001$, Kruskal–Wallis one-way analysis of variance on ranks) at predetermined observation points. Multiple comparison with the Student–Newman–Keuls test revealed significant differences of RNFL reflectance and thickness changes at predetermined loci ($P < 0.05$) (A) Resolution of the macular edema resulted in significant decrease in the thickness of the RNFL at the peak point of the cyst (P), at its nasal edge (N), and 500 μm nasal to the cyst (N500) (*shaded zones*). (B) Significant RNFL reflectance changes were observed after the resolution of the macular edema ($P < 0.001$). RNFL reflectance decreased significantly at the edema's peak ($P = 0.037$), nasal border ($P = 0.02$), and 1500 μm ($P = 0.022$) away from the temporal edge (*shaded zones*). Bars represent the standard error.

was because of the reflection from the RPE-Bruch's membrane segment. Decrease in RNFL reflectance was often accompanied by the appearance of small hyperreflective small dots within the RNFL (Fig. 3D). At preselected areas in the control scans, no significant change was observed in the thickness and reflectance of the RNFL after anti-VEGF injection (data not shown).

Unlike the RNFL thickness change, retinal thickness decreased significantly in a broader zone between points T and N500 after anti-VEGF treatment (Fig. 5). Changes in total retinal thickness after anti-VEGF

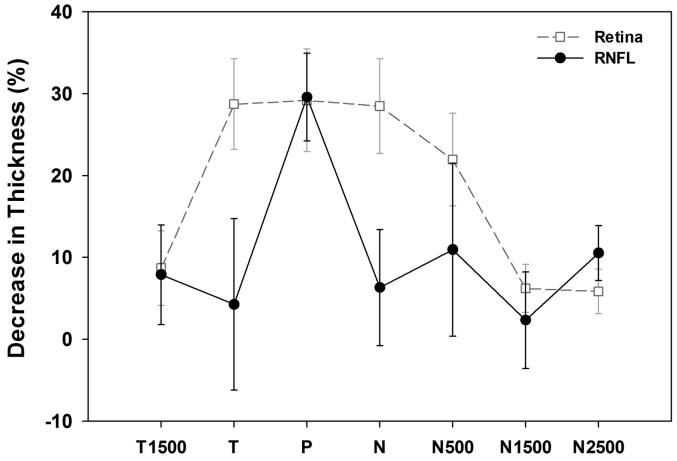

Figure 5. Retinal and RNFL thickness decrease profile after anti-VEGF treatment. Anti-VEGF treatment resulted in a widespread decrease in retinal thickness (gray line) over the macular edema, whereas RNFL thickness changes were centered at the peak point (P) of the macular edema where compression of the axons was the greatest. No spatial correlations were found between the decrease in the thicknesses of the retina and RNFL at any of the preselected points ($P > 0.05$, Spearman rank-order correlation). Bars represent the standard error.

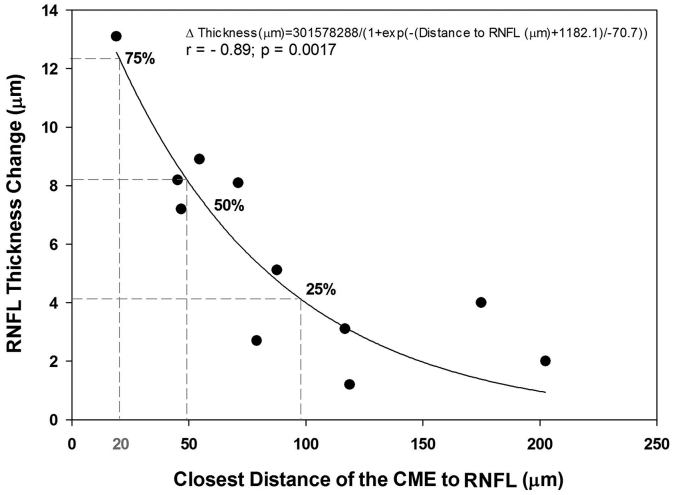

Figure 6. Impact of the proximity of the intraretinal cysts to RNFL thickness. Decrease in RNFL thickness after the resolution of the retinal cysts was negatively correlated (r, –0.89; $P = 0.0017$) with the proximity of the cysts to RNFL. The critical distance (D_{50}) for exertion of this compressive effect was 50 μm.

injection were not correlated with the RNFL thickness changes at any of the preselected loci (Table 2). Among the various anatomic variables of the macular edema analyzed, only the proximity of the intraretinal fluid pockets to RNFL at the peak point (P) significantly correlated with the magnitude of the RNFL thinning at that point ($P = 0.001$; Table 2).

The correlation between the proximity of the cysts to RNFL and the amount of RNFL thinning fit to a sigmoidal curve with the critical distance (D_{50}) of the intraretinal cysts being 50 μm away from the RNFL ($r = 0.89$; $P = 0.002$; Fig. 6).

Discussion

This study demonstrates that, in the presence of macular edema, specific topographic changes of the macular RNFL occur secondary to active compressional strain from the macular cysts on the overlying RNFL. The focal nature of this phenomenon within the macula may explain previously reported inconsistent findings in studies in which correlation of macular edema with peripapillary,[32,33] rather than macular[34,35] RNFL thickness was sought. The absence of similar RNFL changes in nonedematous portions of the macula or in the fellow eye indicate that these changes are neither due to anti-VEGF injections nor to underlying retinal vascular diseases, nor a systemic vasculopathy. One plausible explanation can be leakage of the increased interstitial fluid into the axons, resulting in axonal swelling. Unlike other nerve axons, prelaminar retinal axons are not isolated from the surrounding tissue by a lipid-rich myelin sheath.[36] However, they are wrapped by the processes of Müller cells and astrocytes, which also form the inner retinal barrier.[37] These glial cells establish tight junctions and prevent fluid ingress into the axons.[38] Breakdown of this barrier, although possible, should manifest itself with symmetric swelling of the RNFL on both sides of the peak point along with a decrease in RNFL reflectivity. However, thickening of the RNFL occurs focally at and nasal to the peak site of compression, and accompanied by an increase in RNFL reflectance. The time-course, focal nature and asymmetrical presentations of these changes around the peak point of the macular edema likely indicate axonal stasis, which manifests itself with pooling of hyperreflective intracellular organelles, such as mitochondria and neurofilaments nasal to the site of compression, similar to events that follow pharmacologic stagnation of axoplasmic flow in vitro.[39,40] Asymmetric nasal thickening of the RNFL around the peak point is consistent with constriction of the axons at the lamina cribrosa in patients with glaucoma[41] and animal models of axoplasmic stagnation.[40] Asymmetrical thickening of RNFL can be explained by the known axonal traffic physiology and a consequence of the higher bulk flow rate of retrograde axoplasmic flow compared with anterograde flow. More than 80% of the anterograde axoplasmic flow occurs at a slow speed of 1 to 3 mm

Table 2. Correlation of OCT Parameters with the Decrease in RNFL Thickness After Anti-VEGF Therapy

Decrease in RNFL Thickness	Total Cyst Area	Proximity of the Cysts to RNFL	Horizontal Diameter of the Cyst	Vertical Diameter of the Cyst	Change in RNFL Reflectance	Change in Total Retinal Thickness
POINT P						
β	0.477	0.854	0.47	–0.406	0.017	–0.122
R^2	0.227	0.729	0.221	0.165	0	0.015
p	0.138	0.001*	0.145	0.216	0.962	0.72
POINT N						
β	0.259	0.516	0.271	–0.056	0.231	–0.058
R^2	0.067	0.266	0.073	0.003	0.054	0.003
p	0.442	0.104	0.421	0.871	0.493	0.866
POINT N500						
β	0.138	0.069	0.36	0.057	0.035	–0.144
R^2	0.019	0.005	0.13	0.03	0.001	0.021
p	0.685	0.841	0.276	0.869	0.918	0.673
POINT N1000						
β	0.337	–0.047	0.346	0.375	0.356	0.382
R^2	0.114	0.002	0.12	0.14	0.127	0.146
p	0.311	0.892	0.297	0.256	0.283	0.246
POINT N1500						
β	0.114	–0.086	0.096	0.366	0.032	0.579
R^2	0.013	0.007	0.009	0.134	0.001	0.336
p	0.738	0.802	0.778	0.269	0.925	0.062
POINT T						
β	0.159	0.456	0.102	–0.185	0.555	–0.114
R^2	0.025	0.208	0.01	0.034	0.309	0.013
p	0.641	0.159	0.764	0.585	0.076	0.738
POINT T1500						
β	–0.256	–0.198	–0.244	0.035	–0.145	–0.037
R^2	0.066	0.039	0.06	0.001	0.021	0.001
p	0.447	0.56	0.469	0.918	0.67	0.913

*Spearman rank-order correlation test.

per day, whereas the rest travels with a minority fast component at 150 to 250 mm per day.[42] In contrast, retrograde flow occurs at a uniform speed of 60 to 130 mm per day.[42] Volume correlates of the axoplasmic flow data can be derived to estimate the impact of axonal compression by macular edema. For this reason, flow speed data can be converted to more comparable bulk flow rates, considering that (1) 85% of axoplasm is made up of water[43]; (2) both anterograde and retrograde axoplasmic flow runs within the same axon; and (3) up to 50% of the constituents of the retrograde flow are previously anterograde transported organelles and proteins returning back to ganglion cell soma,[44] which makes the density of fluid running in both directions comparable. With these assumptions in mind, flow rate (Q) in both directions then can be expressed as:

$$Q = \frac{Distance}{Time} = \frac{Area \times Length}{Time} = Area \times Velocity$$

Because the cross-sectional area of the axon is the same for both directions, comparison of the compounded velocity of the anterograde flow to retrograde flow velocity reveals that the volume of retrograde flow is approximately 1.4 to 4.7 times higher than the anterograde flow. Thus more accumulation on the nasal site of the peak compression is a natural consequence of greater volumes of axoplasm arriving to the compression site nasally. Resolution of the macular edema caused more reduction in the thickness of the RNFL at and 500 µm away from the nasal

edge of the cysts compared with segments that are more distant. This is simply because of nonuniform distribution of the intra-axonal pressure gradient and axonal wall stress around the peak of the macular edema.[45] Axonal segments closer to the peak of the macular edema distend more due to higher pressures and exhibited a greater reduction once the compression is resolved. Although the nasal RNFL is physiologically thicker than the temporal RNFL, we failed to detect any significant reduction in the thicknesses of the nasal RNFL above or below the cyst area after the resolution of the cysts, suggesting that increased thickening of the RNFL is not merely due to a baseline thicker RNFL.

RNFL reflectivity changes at and around the peak point of the macular edema also indicate a compressional axoplasmic stagnation by intraretinal cysts. Reflectance of RNFL is a result of light scattering by microtubules, neurofilaments, axonal membranes, and mitochondria within the axon.[16] Distention of the inner retina toward the vitreous due to mechanical compression of the cysts inevitably distorts the RNFL trajectory and may change the angular light scattering of the RNFL at around the peak point.[16] However, RNFL reflectance also manifests itself asymmetrically with larger increases in reflectance occurring nasal to the peak point. Increase in RNFL reflectance may be because of the entrapment of the mitochondria around the most compressed part of the axon. Obviously, this accumulation is expected to occur more on the nasal side because of the higher retrograde axoplasmic flow compared with the anterograde flow. With their 1- to 2-µm-long ellipsoid shape and 0.1 to 0.2 µm thickness, mitochondria are the biggest particles travelling with in the axons. Histopathology of the macular edema also confirms the accumulation of mitochondria within the axons.[46] Similar mitochondrial accumulation is also noted in glaucoma at the prelaminar region optic nerve where axonal compression occurs.[41] We believe the cause of the increased RNFL reflectance is the buildup of highly light-reflective mitochondria,[47] mainly on the nasal side of the macular edema peak. Relieving mechanical pressure on the RNFL with anti-VEGF treatment results in restoration of axoplasmic flow and a decrease in RNFL reflectance on the nasal side of the compressive point. We also observed a decrease in the RNFL reflectivity 1500 µm away from the peak of the macular edema temporally. Keeping in mind the Poiseuille law of fluid dynamics,[48] it is tempting to speculate that resistance created at the peak of the macular edema might have decreased slow anterograde flow below a critical level on the far temporal side, which might have failed to create enough thrust to move the mitochondria further distally. Restoration of the anterograde flow after anti-VEGF treatment might have resolved the stagnation of the mitochondria on the far temporal side and caused the decrease in RNFL reflectance. An interesting observation was the appearance of hyperreflective specks within the RNFL once the mechanical compression of the cysts was relieved. Although the exact nature of this hyperreflective dots is yet to be determined, we believe that they represent aggregates of macromolecules, such as actin, myosin, and calmodulin, similar to axonal spheroids seen in various neurodegenerations.[49] These aggregates are known to occur with the stagnation of the axoplasmic flow and become more distinct after the restoration of the axoplasmic flow and decrease in overall reflectivity of the RFNL. Despite the effect of anti-VEGF treatment on RNFL reflectivity, we did not observe a significant change in the reflectivity of the retinal tissues below RNFL after the resolution of intraretinal cysts. This observation is not surprising considering that 78.2% ± 5.6% reflectance values below RNFL is generated by RPE-Bruch's membrane complex, which is not primarily affected from macular edema. However, our observation may also be the result of early inner retinal atrophy that develops during the course of cystoid macular edema.

In addition to the topographic changes described earlier, we also showed that the only variable that was significantly associated with the magnitude of RNFL thickness changes was the proximity of the peak of the macular cysts to the RNFL. Similar observations were reported indirectly through correlating the size of the cystoid macular edema to the visual outcome.[50] From a mechanical point of view, one may assume that compression and deformation of the RNFL would be greater in magnitude if there is less intervening retinal tissue between the cyst and the RNFL to buffer the physical strain applied by the cysts. The closer the cyst to the RNFL, the larger the percent decompression achieved from treating with anti-VEGF therapy, suggesting that the proximity of the cysts to the RNFL may be a consideration in the decision to treat. The 50th percentile of the pressure-relieving effect of anti-VEGF treatment corresponded to 50 µm distance proximity of the cyst peaks to RNFL; that is, on average, a 50% reduction in RNFL cyst-induced thickening can be expected if the peak of the cystic area is 50 µm away from the RNFL prior to injection.

Focal nature of the RNFL changes and their temporal relationship with the disappearance of the intraretinal cysts after anti-VEGF treatment strongly suggest that the short-term RNFL thinning seen with anti-VEGF use is a result of immediate decompression of axonal stasis caused by presence of macular edema, rather than axonal loss. However, definite proof of this

conclusion will require functional tests, such as visual field analyses or histopathological verification. A previous transmission electron microscopy study supports our observation by demonstration axonal compression by intraretinal cysts in two eyes.[46] Our study only analyzes short-term changes over the course of approximately 1 to 2 months post-anti-VEGF therapy, allowing us to isolate specifically the effects of acute compression from macular edema. We cannot rule out long-term mechanisms that affect RNFL thickness or axonal numbers. For example, the DRCR Protocol S study demonstrated RNFL thinning in eyes both with and without DME that were treated with anti-VEGF therapy,[14] however their observation period spanned 2 years rather than 1 or 2 months, likely implicating the impact of many other factors in addition to compression on RNFL thickness and axon number.

Poorly controlled RNFL compression and axonal stasis seen in other compressive pathologies, such as acute angle closure and optic disc edema, also lead to eventual RNFL atrophy and axonal loss. The focal compressive effects that we see with macular edema are likely to have similar effects on the area of compressed RNFL in the long term, and may explain the focal RNFL atrophy seen along with macular edema in both DME[51] and retinal vein occlusion cases.[52] The magnitude of this compression can be better understood comparing it with the compression of retinal axons at lamina cribrosa by increased intraocular pressure in patients with glaucoma. For this purpose, we created a mathematical model of focal axonal compression by macular edema and estimated the compressive force exerted focally on the overlying RNFL (Fig. 7). Using this mathematical model, we estimated that focal compression of the axons at the peak of the macular edema can create compressive forces equivalent to the forces experienced by the RNFL in an eye with an intraocular pressure of up to 62 mm Hg (Fig. 7) Longer duration of this compression is probably one of the major reasons resulting in failure in regaining baseline sight after resolution of the edema.[53]

Our findings, although clinically important, must be interpreted with caution and a number of limitations must be borne in mind. The first is the several structural changes that may occur in diabetic retinopathy and retinal vein occlusion along with macular edema, which may have an impact on the integrity of the RNFL. To overcome this difficulty, we applied strict screening criteria to isolate the effects cystoid macular edema on RNFL. For this purpose, we excluded patients with proliferative diabetic retinopathy, macular ischemia, media opacities, and/or any other condition that may affect RNFL integrity. As a result, we were able to include only 11 eyes of 10 patients out of 117 screened patients. Although we believe that by applying our criteria, we eliminate the several confounding factors, we cannot exclude the possibility that some unseen pathologies might have had an impact on our results. The retrospective nature of the study also carries forward all inherited weaknesses, such as difficulty in assessing the temporal relationship between the macular edema and axonal stasis, or the impact of repeated injections on axonal integrity in the long-term. However, overcoming such difficulties in a prospective trial in a similar setting will also be a challenge.

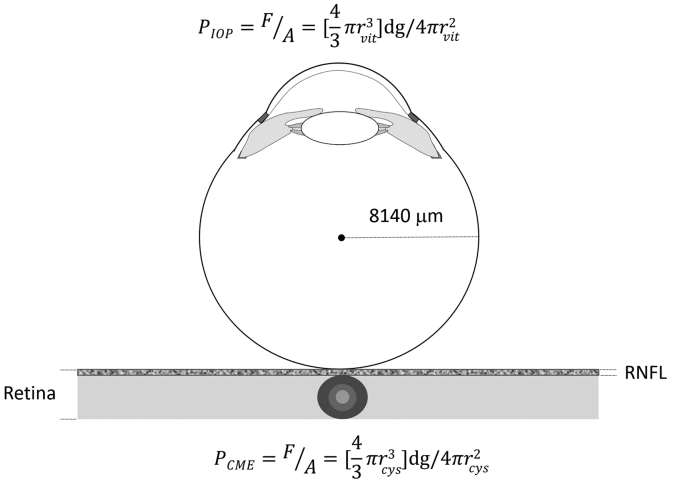

Figure 7. Mathematical model for estimating the magnitude of pressure exerted by intraretinal cysts. Inward deflection of the retina over the cysts indicates that the pressure exerted by the intraretinal fluid pockets is greater than the intraocular pressure. The magnitude of this pressure is equal to the force (F) applied per unit area (A). Considering the spherical shape of intraretinal cysts as a single body, pressure applied by the cysts on the RNFL (P_{CME}) can then be calculated as: $[4/3\ \pi r_{cyst}^{3}]$ x d x g/ $4\ \pi r_{cyst}^{2}$ where (d) denotes the density of the water and (g) is the gravitational constant. Similarly, the outward pressure on RNFL exerted by intraocular pressure (P_{IOP}) is equal to $[4/3\ \pi r_{vitreous}^{3}]$ x d x g/ $4\ \pi r_{vitreous}^{2}$. Simplification of the formulas will reveal that the ratio of the radii of the vitreous cavity ($r_{vitreous}$) and intraretinal cysts (r_{cyst}) will yield the quotient of the opposing pressures (P_{IOP}/P_{CME}). Substituting the numeric value of the vitreous radius (16.28 mm)[57] and using the average diameter of the cysts observed in this study (264.5 ± 78.4 µm) indicate that the force applied by the intraretinal cysts is comparable to an increase in intraocular pressure up to 62 mm Hg.

Conclusions

Thus we believe compression and deformation of the RNFL by volumetric expansion of the intraretinal cysts is a common but overlooked phenomenon because of the plethora of clinical findings patients

present to physicians. Patients with good visual acuity (>20/30) and macular edema may be reluctant to treatment and physicians may prefer to observe the patient.[54–56] However, it may be clinically prudent to relieve promptly this compressional axonal stasis with anti-VEGF therapy before axonal atrophy develops, especially in patients who have low axonal reserve, such as those with preexisting glaucoma or macular ischemia due to vascular pathologies. This holds especially true for macular edema with cysts in close proximity (<50 µm) to the RNFL, given that effective compression in these cases is of greater detrimental effect.

Acknowledgments

Supported in part by an unrestricted grant from Research to Prevent Blindness, Inc., New York, NY, USA, Slomo and Cindy Silvian Foundation, New York, NY, USA, and TUBITAK, Ankara, Turkey.

Presented in part at the Annual Meeting of the Retina Society, San Francisco, CA, USA, September 2018.

Disclosure: **E. Karahan,** None; **A. Abdelhakim,** None; **C. Durmaz,** None; **T.H. Tezel,** None

References

1. Papadopoulos N, Martin J, Ruan Q, et al. Binding and neutralization of vascular endothelial growth factor (VEGF) and related ligands by VEGF Trap, ranibizumab and bevacizumab. *Angiogenesis*. 2012;15:171–185.
2. Hernandez C, Dal Monte M, Simo R, Casini G. Neuroprotection as a therapeutic target for diabetic retinopathy. *J Diabetes Res*. 2016;2016:9508541.
3. Amato R, Biagioni M, Cammalleri M, Dal Monte M, Casini G. VEGF as a survival factor in ex vivo models of early diabetic retinopathy. *Invest Ophthalmol Vis Sci*. 2016;57:3066–3076.
4. Foxton RH, Finkelstein A, Vijay S, et al. VEGF-A is necessary and sufficient for retinal neuroprotection in models of experimental glaucoma. *Am J Pathol*. 2013;182:1379–1390.
5. Shen J, Xiao R, Bair J, et al. Novel engineered, membrane-localized variants of vascular endothelial growth factor (VEGF) protect retinal ganglion cells: a proof-of-concept study. *Cell Death Dis*. 2018;9:1018.
6. Saleh R, Karpe A, Zinkernagel MS, Munk MR. Inner retinal layer change in glaucoma patients receiving anti-VEGF for neovascular age related macular degeneration. *Graefes Arch Clin Exp Ophthalmol*. 2017;255:817–824.
7. Lee WJ, Kim YK, Kim YW, et al. Rate of macular ganglion cell-inner plexiform layer thinning in glaucomatous eyes with vascular endothelial growth factor inhibition. *J Glaucoma*. 2017;26:980–986.
8. Nishijima K, Ng YS, Zhong L, et al. Vascular endothelial growth factor-A is a survival factor for retinal neurons and a critical neuroprotectant during the adaptive response to ischemic injury. *Am J Pathol*. 2007;171:53–67.
9. Lee JM, Bae HW, Lee SY, Seong GJ, Kim CY. Effect of anti-vascular endothelial growth factor antibody on the survival of cultured retinal ganglion cells. *Korean J Ophthalmol*. 2017;31:360–365.
10. Foxton R, Osborne A, Martin KR, Ng YS, Shima DT. Distal retinal ganglion cell axon transport loss and activation of p38 MAPK stress pathway following VEGF-A antagonism. *Cell Death Dis*. 2016;7:e2212.
11. Spitzer MS, Wallenfels-Thilo B, Sierra A, et al. Antiproliferative and cytotoxic properties of bevacizumab on different ocular cells. *Br J Ophthalmol*. 2006;90:1316–1321.
12. Shin HJ, Shin KC, Chung H, Kim HC. Change of retinal nerve fiber layer thickness in various retinal diseases treated with multiple intravitreal antivascular endothelial growth factor. *Invest Ophthalmol Vis Sci*. 2014;55:2403–2411.
13. Shin HJ, Kim SN, Chung H, Kim TE, Kim HC. Intravitreal anti-vascular endothelial growth factor therapy and retinal nerve fiber layer loss in eyes with age-related macular degeneration: a meta-analysis. *Invest Ophthalmol Vis Sci*. 2016;57:1798–1806.
14. Jampol LM, Odia I, Glassman AR, et al. Panretinal photocoagulation versus ranibizumab for proliferative diabetic retinopathy: comparison of peripapillary retinal nerve fiber layer thickness in a randomized clinical trial. *Retina*. 2019;39:69–78.
15. Logroscino CA, Sanguinetti C, Catalano F. Electron microscopic study of the early changes proximal to a constriction in myelinated nerve. *Int Orthop*. 1980;4:121–125.
16. Zhou Q, Knighton RW. Light scattering and form birefringence of parallel cylindrical arrays that represent cellular organelles of the retinal nerve fiber layer. *Appl Opt*. 1997;36:2273–2285.
17. Lee KM, Woo SJ, Hwang JM. Differentiation of optic nerve head drusen and optic disc edema

with spectral-domain optical coherence tomography. *Ophthalmology*. 2011;118:971–977.
18. Albrecht P, Blasberg C, Ringelstein M, et al. Optical coherence tomography for the diagnosis and monitoring of idiopathic intracranial hypertension. *J Neurol*. 2017;264:1370–1380.
19. Jin SW, Lee SM. Comparison of longitudinal changes in circumpapillary retinal nerve fiber layer and ganglion cell complex thickness after acute primary angle closure: a 12-month prospective study. *Jpn J Ophthalmol*. 2018;62:194–200.
20. Huang XR, Knighton RW, Zhou Y, Zhao XP. Reflectance speckle of retinal nerve fiber layer reveals axonal activity. *Invest Ophthalmol Vis Sci*. 2013;54:2616–2623.
21. Alloatti M, Bruno L, Falzone TL. Methods for quantitative analysis of axonal cargo transport. *Methods Mol Biol*. 2018;1727:217–226.
22. Davis MD, Fisher MR, Gangnon RE, et al. Risk factors for high-risk proliferative diabetic retinopathy and severe visual loss: Early Treatment Diabetic Retinopathy Study Report #18. *Invest Ophthalmol Vis Sci*. 1998;39:233–252.
23. Kass MA, Heuer DK, Higginbotham EJ, et al. The Ocular Hypertension Treatment Study: a randomized trial determines that topical ocular hypotensive medication delays or prevents the onset of primary open-angle glaucoma. *Arch Ophthalmol*. 2002;120:701–713; discussion 829–730.
24. Bracha P, Moore NA, Ciulla TA, WuDunn D, Cantor LB. The acute and chronic effects of intravitreal anti-vascular endothelial growth factor injections on intraocular pressure: a review. *Surv Ophthalmol*. 2018;63:281–295.
25. Tseng JJ, Vance SK, Della Torre KE, et al. Sustained increased intraocular pressure related to intravitreal antivascular endothelial growth factor therapy for neovascular age-related macular degeneration. *J Glaucoma*. 2012;21:241–247.
26. Eadie BD, Etminan M, Carleton BC, Maberley DA, Mikelberg FS. Association of repeated intravitreous bevacizumab injections with risk for glaucoma surgery. *JAMA Ophthalmol*. 2017;135:363–368.
27. Classification of diabetic retinopathy from fluorescein angiograms. ETDRS report number 11. Early Treatment Diabetic Retinopathy Study Research Group. *Ophthalmology*. 1991;98(5 suppl):807–822.
28. Hafner J, Prager S, Lammer J, et al. Comparison of ganglion cell inner plexiform layer thickness by Cirrus and Spectralis optical coherence tomography in diabetic macular edema. *Retina*. 2018;38:820–827.
29. Hosseini H, Razeghinejad MR, Nowroozizadeh S, Jafari P, Ashraf H. Effect of macular edema on optical coherence tomography signal strength. *Retina*. 2010;30:1084–1089.
30. Jonas JB, Nguyen XN, Naumann GO. Parapapillary retinal vessel diameter in normal and glaucoma eyes. I. Morphometric data. *Invest Ophthalmol Vis Sci*. 1989;30:1599–1603.
31. Gardiner SK, Demirel S, Reynaud J, Fortune B. Changes in retinal nerve fiber layer reflectance intensity as a predictor of functional progression in glaucoma. *Invest Ophthalmol Vis Sci*. 2016;57:1221–1227.
32. Kim J, Woo SJ, Ahn J, Park KH, Chung H, Park KH. Long-term temporal changes of peripapillary retinal nerve fiber layer thickness before and after panretinal photocoagulation in severe diabetic retinopathy. *Retina*. 2012;32:2052–2060.
33. Hwang DJ, Lee EJ, Lee SY, Park KH, Woo SJ. Effect of diabetic macular edema on peripapillary retinal nerve fiber layer thickness profiles. *Invest Ophthalmol Vis Sci*. 2014;55:4213–4219.
34. Yang HS, Woo JE, Kim MH, Kim DY, Yoon YH. Co-evaluation of peripapillary RNFL thickness and retinal thickness in patients with diabetic macular edema: RNFL misinterpretation and its adjustment. *PLoS One*. 2017;12:e0170341.
35. Jo YJ, Kim WJ, Shin IH, Kim JY. Longitudinal changes in retinal nerve fiber layer thickness after intravitreal anti-vascular endothelial growth factor therapy. *Korean J Ophthalmol*. 2016;30:114–120.
36. Denninger AR, Breglio A, Maheras KJ, et al. Claudin-11 tight junctions in myelin are a barrier to diffusion and lack strong adhesive properties. *Biophys J*. 2015;109:1387–1397.
37. Bauer H, Stelzhammer W, Fuchs R, et al. Astrocytes and neurons express the tight junction-specific protein occludin in vitro. *Exp Cell Res*. 1999;250:434–438.
38. Garcia-Pradas L, Gleiser C, Wizenmann A, Wolburg H, Mack AF. Glial cells in the fish retinal nerve fiber layer form tight junctions, separating and surrounding axons. *Front Mol Neurosci*. 2018;11:367.
39. Edmonds BT, Koenig E. ATP and calmodulin dependent actomyosin aggregates induced by cytochalasin D in goldfish retinal ganglion cell axons in vitro. *J Neurobiol*. 1990;21:555–566.
40. Kano M, Tashiro H, Kawakami T, Takenaka T, Gotoh H. Differential suppression of axoplasmic transport: effects of light irradiation to the growth

cone of cultured dorsal root ganglion neurons. *Cell Mol Neurobiol*. 1995;15:297–306.
41. Hollander H, Makarov F, Stefani FH, Stone J. Evidence of constriction of optic nerve axons at the lamina cribrosa in the normotensive eye in humans and other mammals. *Ophthalmic Res*. 1995;27:296–309.
42. Hayreh SS. Fluids in the anterior part of the optic nerve in health and disease. *Surv Ophthalmol*. 1978;23:1–25.
43. Weiss P, Hiscoe HB. Experiments on the mechanism of nerve growth. *J Exp Zool*. 1948;107:315–395.
44. Edstrom A, Hanson M. Retrograde axonal transport of proteins in vitro in frog sciatic nerves. *Brain Res*. 1973;61:311–320.
45. Chow JF, Soda K. Laminar flow in tubes with constriction. *Phys Fluids*. 1972;15:1700–1706.
46. Yanoff M, Fine BS, Brucker AJ, Eagle RC, Jr. Pathology of human cystoid macular edema. *Surv Ophthalmol*. 1984;28(suppl):505–511.
47. Thar R, Kuhl M. Propagation of electromagnetic radiation in mitochondria? *J Theor Biol*. 2004;230:261–270.
48. Pfitzner J. Poiseuille and his law. *Anaesthesia*. 1976;31:273–275.
49. Beirowski B, Nogradi A, Babetto E, Garcia-Alias G, Coleman MP. Mechanisms of axonal spheroid formation in central nervous system Wallerian degeneration. *J Neuropathol Exp Neurol*. 2010;69:455–472.
50. Katome T, Mitamura Y, Nagasawa T, Eguchi H, Naito T. Quantitative analysis of cystoid macular edema using scanning laser ophthalmoscope in modified dark-field imaging. *Retina*. 2012;32:1892–1899.
51. Bonnin S, Tadayoni R, Erginay A, Massin P, Dupas B. Correlation between ganglion cell layer thinning and poor visual function after resolution of diabetic macular edema. *Invest Ophthalmol Vis Sci*. 2015;56:978–982.
52. Kim HJ, Yoon HG, Kim ST. Correlation between macular ganglion cell-inner plexiform layer thickness and visual acuity after resolution of the macular edema secondary to central retinal vein occlusion. *Int J Ophthalmol*. 2018;11:256–261.
53. Yeh WS, Haller JA, Lanzetta P, et al. Effect of the duration of macular edema on clinical outcomes in retinal vein occlusion treated with dexamethasone intravitreal implant. *Ophthalmology*. 2012;119:1190–1198.
54. Ferris FL, Davis MD, 3rd. Treating 20/20 eyes with diabetic macular edema. *Arch Ophthalmol*. 1999;117:675–676.
55. Diabetic Retinopathy Clinical Research Network,Writing C ommittee, Aiello LP, et al. Rationale for the diabetic retinopathy clinical research network treatment protocol for center-involved diabetic macular edema. *Ophthalmology*. 2011;118:e5–e14.
56. Das T, Aurora A, Chhablani J, et al. Evidence-based review of diabetic macular edema management: consensus statement on Indian treatment guidelines. *Indian J Ophthalmol*. 2016;64:14–25.
57. Atchison DA, Thibos LN. Optical models of the human eye. *Clin Exp Optom*. 2016;99:99–106.